小型電気自動車 … に関する研究
(ABS に対す … 制御の効果)

Research on Skid Control System of Small Electric Vehicle

(The Effect of Regenerative Brake Control on In-Wheel Small Electric Vehicle with Anti-Lock Brake System)

1 April 2011 ~ 1 April 2013

Muhammad Izhar Ishak*
*Graduate School of Mechanical Engineering, Department of Mechanical Engineering, Tokai University Shonan Campus
4-1-1 Kitakaname, Hiratsuka City, Kanagawa, JAPAN

Dr. Eng. Hirohiko Ogino**
**Department of Prime Mover Engineering, Faculty of Mechanical Engineering, Tokai University Shonan Campus

CONTENT

INTRODUCTION

During this recent years, concerns over the environmental impact by petroleum based transportation, along with the issue of peak oil, has led to renewed interest over electric mode of transportation. Japan automobile companies are said to be the leader of today's development in manufacturing electric vehicle.

The fundamental of driving method for electric vehicle can be separated into two types; which are one motor system and in-wheel motor system. It is believe that in-wheel motor system has tremendous potential in the future of EV as it is very small and has the advantage towards row transfer loss of energy. In-wheel motor is also the key to this research in the establishment of all-wheel independent steering system as it offers more freedom of movement to the wheel from all-wheel drive.

As the world progress in the usage of electrical based transportation, the demand on the research on stability, controllability and feasibility of electric vehicle simultaneously increases. The components of a conventional vehicle that consist of mechanical links schema will be altered into electrical module schema which only connected by signal cable. This electric powered and by-wire control technology downsizing a major mechanical parts and permits freedom of layout and potential. Due to this reason, four wheels independent steering system for electric vehicle is much more accomplishable compared to conventional vehicle bound to mechanical constrains.

One question that must be considered is whether small electric vehicles are sufficiently safe to drive. Most small in-wheel motor electric vehicles only provide seat belts as safety equipment and does not have an antilock braking system [2] or a traction control system, which are basic skid control systems, because an in-wheel motor system is used as the driving unit. For the same reason, small in-wheel motor electric vehicles employ a mechanical braking system rather than a hydraulic braking system. Although the mechanical brake system is compact, the stiffness of the system is smaller than that of the hydraulic braking system, and the response performance of the braking force of the mechanical system is low. As such, small electric vehicles may be considered to provide insufficient safety.

Recently there has been many researches that shows simulation of an ABS can be combined with a hydraulic-mechanical hybrid brake system [(3) ~ (9)] on a two wheel drive (2WD) small electric vehicle as a basic skid control system. Despite the discovery, ABS has still not been available for small in-wheel motor electric vehicles until today.

The long term of this research is a development of four wheel independent steering (4WS) for in-wheel small electric vehicle based on steering performance. Before an actual vehicle can be achieved, a complex mathematical model has to be constructed to manifest the vehicle's dynamic for four wheel drive (4WD) and four wheel steering (4WS). The complex model is then compared to experimental results as a confirmation. Due to dangerous driving and hazardous conditions, the confirmation by experiments has to be done by a simple computation model.

In this research, the complex mathematical model for 4WS was done by investigation of an in-wheel small electric vehicle with hydraulic-mechanical hybrid brake systems based on steering performance. The model of this small electric vehicle used has a rear in-wheel motor system that produced a regenerative brake and utilizing a mechanical brake system. The objective of this research is to investigate the effectiveness of ABS of a small electric vehicle operating a hybrid hydraulic-mechanical brake system during braking on conditional road, and the influence over regenerative brake on rear wheel. The experimental results are performed using a numerical simulation.

OBJECTIVE

In the conventional diesel and gasoline vehicle, the engine output is delivered to the wheels through several mechanical components include transmission, driveshaft and differential. However, with in-wheel motor, electric power is transferred directly to each wheel via signal cables, eliminating the possibility of energy loss and provides excess free space to install other components such as servo motor which is needed to steer the wheel independently.

The objective of this research is to validate a control method for complex mathematical model of a four wheel steering small electric vehicle by investigating the steering performance during braking of a two wheel drive (2WD) small electric vehicle with hydraulic mechanical hybrid brake system. A 2WD small electric vehicle was used to determine all possible parameters that are going to be used throughout the research. Due to only braking condition is taken consideration, an anti-lock brake systems was evaluated as a basic skid control system.

In order to achieve the objective, investigations was done by using a Visual Studio numerical simulation. The current electric vehicle (Toyota COMS) features was used as a model in the simulation. A few alterations were made in the simulation whereas the current EV was not equipped with an ABS. The experimental result of the steering performance during different road; which was dry asphalt and icy road, and driving condition was evaluated to set the parameters and acquires the proper control method.

IN-WHEEL MOTOR

The name 'in-wheel motor' self-explains the meaning of the machine. It is an electric motor that incorporates into the unused wheel hub of a vehicle and provides driving propulsion by electricity. The amount of power generated by in-wheel motor can vary depending on the size of the motor.

One of the great advantages of in-wheel electric motor system is that it has high energy efficiency. The electric power transmitted from the driver goes straight to the wheel via electric cables, reducing the distance and medium the power travel increase the efficiency of energy. For example, in a hectic traffic condition, a conventional internal combustion engine may only provide 20% of energy efficiency due to energy lost by mechanical parts and surroundings such as heat. However, in a same condition, an in-wheel motor can provide up to 90% of energy efficiency.

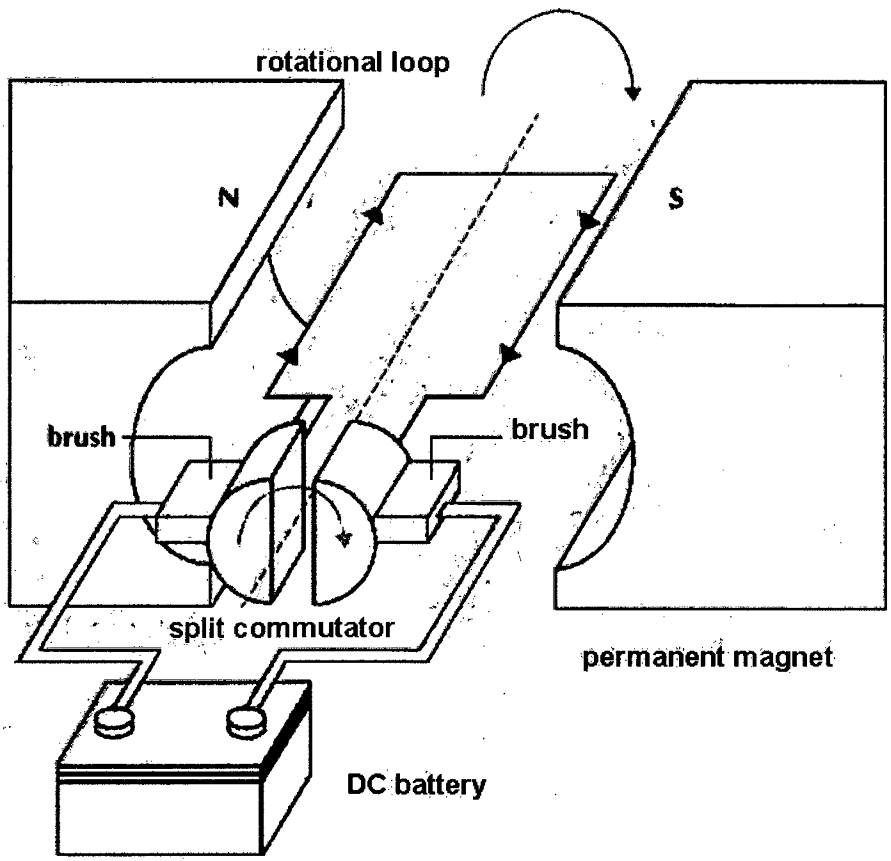

Figure 1: Simple brush electric motor

Electric motor is one of the most important applications in the relationship between electricity and magnetism. Figure 1 illustrates a simple and basic structure of an electric motor to explain the mechanism of an electric motor. When an electric current is passed through a circuit, this will create a magnetic field around the wire which interacts with the magnetic field of the permanent magnet. The brush makes sure that the current flows in one direction to produce a rotation loop. This is called an electric brush motor.

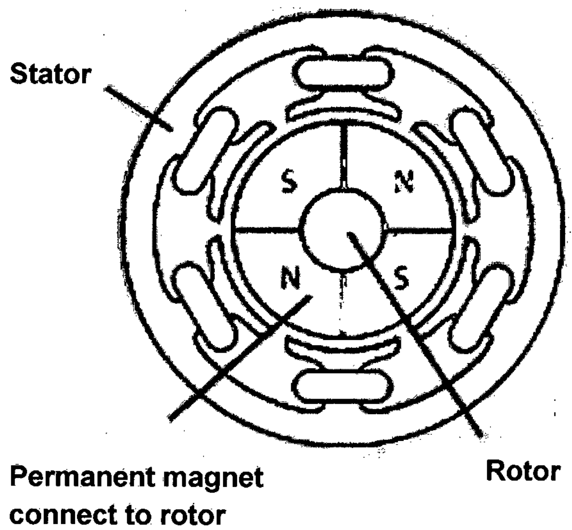

Figure 2: Brushless electric motor

The electric motor of an in-wheel small electric vehicle is different. Instead of the electric circuit, the moving part in the middle is consisting of one or more permanent magnets as shown in figure 2. This type of motor is called electric brushless motor. A brushless motor is much more precise rotation, higher efficiency, and more torque per weight.

ANTI-LOCK BRAKE SYSTEM (ABS)

Anti-lock brake system (ABS) is one of the skid control system in automobile that allows the wheels of a vehicle to maintain traction with the surface of the road disregarding the drivers braking force preventing the wheels from locking up or stop rotating while the vehicle is still in motion. ABS offers a huge improvement in vehicle stability and maneuverability and decrease stopping distances on dry and slippery road conditions. Figure 3 shows the simple structure of an ABS unit.

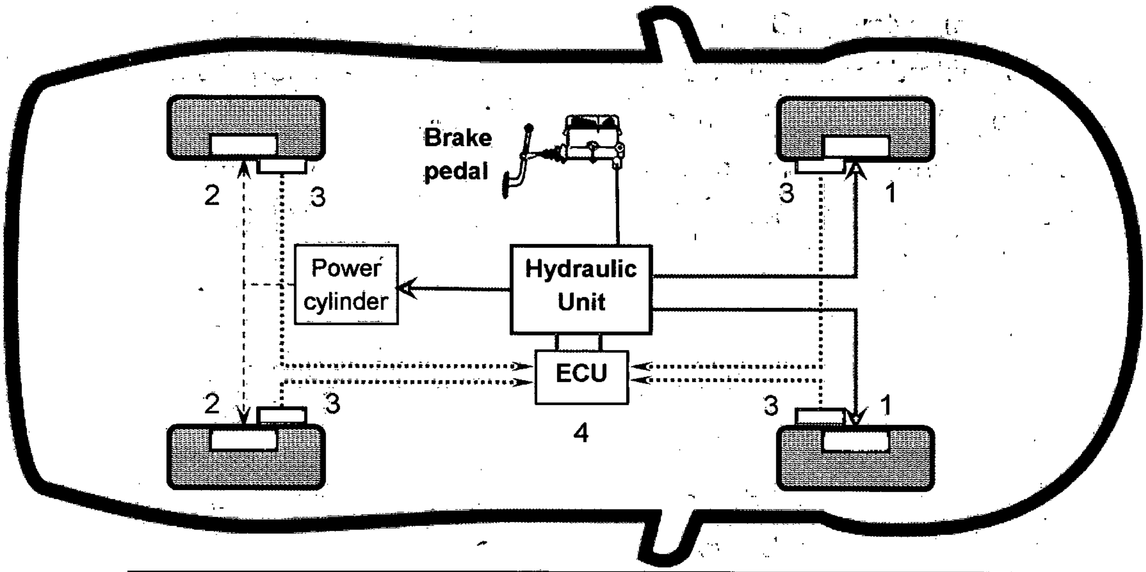

1: hydraulic brake line, 2: mechanical linkage, 3: signal cable connection to speed sensor, 4: electric control unit

Figure 3: ABS Unit

Speed Sensor

In order for the anti-lock brake system to supervise the wheel during lock up, a speed sensor located on each wheel is need.

Electronic Control Unit (ECU)

The ECU is the controller in the vehicle which receive feedback from each individual wheel speed sensor, in case if there a variation in the wheel speed causing traction lose the signal is sent to the controller. The controller will then limit the brake force by activate the braking valve on and off.

Hydraulic Unit

The hydraulic consist of three-channel piping model, each piping for the front wheels and one that connects to the power cylinder that controls the mechanical brakes for the rear wheels. The hydraulic unit receives the braking pressure directly from the master cylinder. The separation on the front wheels provides particular control for maximum braking efficiency while the rear wheels are control simultaneously. In the hydraulic unit contains 3 IN-valves, 3 OUT-valves and a piston pump.

- Valve

  The ECU send a signal to the IN and the OUT valve to control the pressure generate from the master cylinder. In normal braking condition, the IN-valves open allowing the pressure from the master cylinder to pass through to the wheel cylinder. However, when the driver pushes the pedal too hard, the IN-valves close isolating the pressure from the master cylinder. And lastly, when in skidding condition the OUT-valves open to release pressure from the wheel cylinder, decreasing the braking force.

- Pump

  When the valves release the pressure from the brakes, the pump is used to regain the pressure back to the wheel cylinder.

ABS Operation

The slip ratio is crucial for the ABS to operate by expressing the traction characteristics between the vehicle's tire and road surface. Equation (1) proposed the definition of slip ratio ρ. Where u indicates the body speed, ω denotes the rotational speed of the tire, and r denotes the radius of the tire.

$$\begin{cases} \rho = \dfrac{u - r\omega}{u} & \text{(braking)} \\ \rho = \dfrac{r\omega - u}{r\omega} & \text{(driving)} \end{cases} \tag{1}$$

By using the value of slip ratio, an approximation of the friction coefficient μ of the tire and the road surface can be calculated in the following equation (2);

$$\begin{cases} \mu = 1.10k \times (e^{35\rho} - e^{0.35\rho}) & \text{(braking)} \\ \mu = -1.05k \times (e^{-45\rho} - e^{-0.45\rho}) & \text{(driving)} \end{cases} \qquad (2)$$

Where k is the parameter of the road condition, for which the values are as follow;

$$\begin{cases} k = 1.0 & \text{(dry asphalt)} \\ k = 0.2 & \text{(icy road)} \end{cases}$$

Utilizing slip ratio and friction coefficient equations, a typical tire characteristic curve is produced as such in figure 4. When the tire is locked, the slip ratio becomes 1.0, and the friction coefficient decreases and becomes approximately zero. As a result, the braking force is reduced, and the motion of the vehicle becomes uncontrollable.

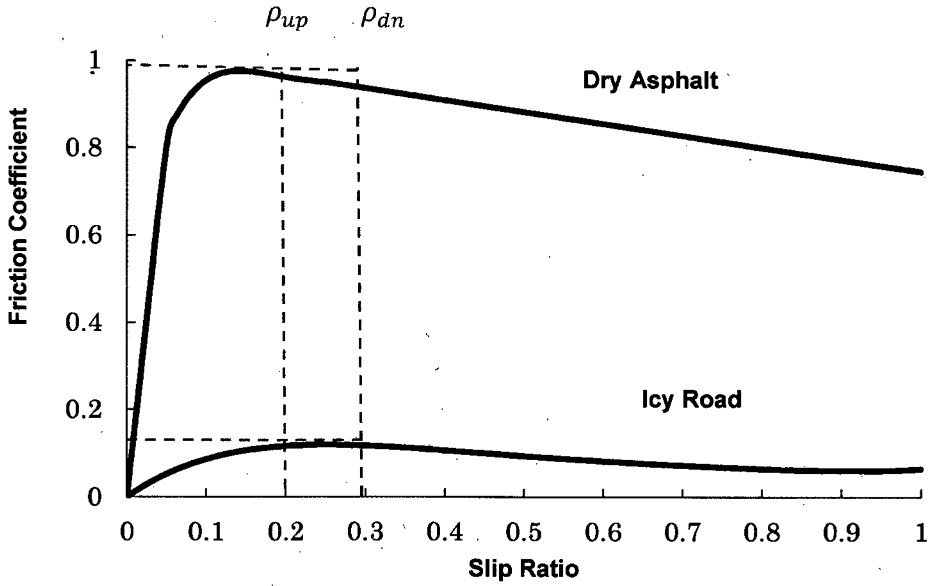

Figure 4: ABS Control Unit by Typical Tire Characteristic

The ABS controls the slip ratio so that the friction coefficient is maximized. When tire lock occurs, i.e., when the slip ratio becomes 1.0, the IN valve is closed, the OUT valve is opened, and the pump begins to operate. The pressure in the wheel cylinder and the braking force are decreased. As a result, the slip ratio becomes small, and the friction co-efficiency and the side force become larger. When the slip ratio becomes too small, the IN valve opens and the OUT valve closes again. The pressures in the wheel cylinder and the braking force are increased, and the slip ratio then becomes large.

It is suggested that in ABS controller unit, when the slip ratio reaches the value between ρ_{up} =0.2 and ρ_{dn} = 0.3, the vehicle can obtain the maximum value of friction coefficient and a high degree of cornering force shown in Figure 4.

VEHICLE BRAKING SYSTEM

Hydraulic-Mechanical Hybrid Brake System

Figure 5 shows the construction of a hydraulic-mechanical brake system represented as two wheel drive vehicle and both left and right side of the brake system have the same mechanism.

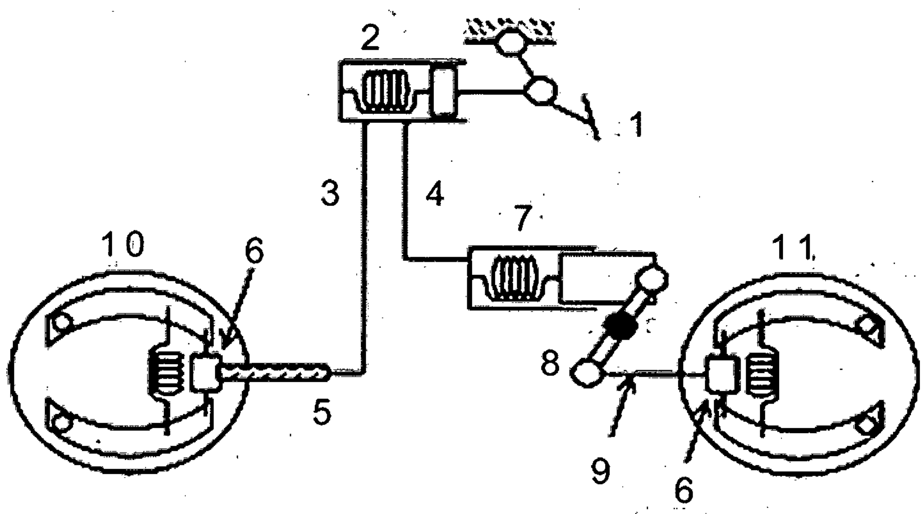

1:Brake Pedal 2:Master Cylinder 3:Front Brake Tube 4:Rear Brake Tube 5:Brake Hose 6:Wheel Cylinder 7:Power Cylinder 8:Link 9:Wire 10:Front Drum Brake 11:Rear Drum Brake

Figure 5: Hydraulic-Mechanical Hybrid Brake System

The front brake system is a hydraulic braking system while the rear brake system is a mechanical braking system. In hydraulic brake system, the braking force of the front drum brake is monotonous to the force acted from master cylinder (M/C) pressure. The total force is defined as equation 3;

$$F_{hydraulic} = (pressure) \times (master\ cylinder\ cross\ section\ area)$$
$$= \rho g H \times \frac{\pi d^2}{4} \quad (3)$$

In mechanical brake system, the braking pressure generated in the master cylinder is directed into a power cylinder. The piston from power cylinder pulls a wire connected to the rear drum brake that moves the brake shoe. Every power cylinder is represented by a spring-mass-damper system and the wire connecting from the power cylinder to the drum brake is represented as a spring. The dynamic force equation from the power cylinder to the wire of a mechanical brake system can be shown in below;

$$m_p \frac{d^2 x_p}{dt^2} = \rho g H A - k_w(x_p - x_d) - k_p x_p - d_p \frac{dx_p}{dt}$$

In the simulation, the displacement of power cylinder spring x_p is calculated by using finite-differential method on the dynamic force equation above. When assuming a uniform partition in time Δt, so the difference between two consecutive spaces is donated as (A) for the first order and (B) second order.

$$m_p \frac{d\dot{x}_p}{dt} = \rho g H A - k_w(x_{p(A)} - x_{d(A)}) - k_p x_{p(A)} - d_p \dot{x}_{p(A)}$$

$$m_p \frac{\dot{x}_{p(B)} - \dot{x}_{p(A)}}{\Delta t} = \rho g H A - k_w(x_{p(A)} - x_{d(A)}) - k_p x_{p(A)} - d_p \dot{x}_{p(A)}$$

Let consider,

$$\Rightarrow \quad F_{tot} = \rho g H A - k_w(x_{p(A)} - x_{d(A)}) - k_p x_{p(A)} - d_p \dot{x}_{p(A)}$$

The velocity of the power cylinder spring,

$$\dot{x}_{p(B)} = \dot{x}_{p(A)} + \frac{\Delta t}{m_p}(F_{tot})$$

Thus the displacement of the spring is

$$\dot{x}_{p(B)} = \frac{dx_p}{dt} = \dot{x}_{p(A)} + \frac{\Delta t}{m_p}(F_{tot})$$

$$\frac{x_{p(B)} - x_{p(A)}}{\Delta t} = \dot{x}_{p(A)} + \frac{\Delta t}{m_p}(F_{tot})$$

$$x_{p(B)} = x_{p(A)} + \Delta t\left(\dot{x}_{p(A)} + \frac{\Delta t}{m_p}(F_{tot})\right)$$

However for the dynamic force equation from the wire to the rear drum brake of a mechanical drum brake system is shown below;

$$m_d\frac{d^2x_d}{dt^2} = k_w(x_p - x_d) - k_d x_d - d_d\frac{dx_d}{dt}$$

In order to calculate the displacement of drum brake spring x_d, the same method of finite-differential was used.

$$m_d\frac{d\dot{x}_d}{dt} = k_w(x_p - x_d) - k_d x_d - d_d\dot{x}_d$$

$$m_d\frac{\dot{x}_{d(B)} - \dot{x}_{d(A)}}{\Delta t} = k_w(x_{p(A)} - x_{d(A)}) - k_d x_{d(A)} - d_d\dot{x}_{d(A)}$$

The velocity of the drum brake spring,

$$\therefore \dot{x}_{d(B)} = \dot{x}_{d(A)} + \frac{\Delta t}{m_d}\left(k_w(x_{p(A)} - x_{d(A)}) - k_d x_{d(A)} - d_d\dot{x}_{d(A)}\right)$$

Thus the displacement of the spring is

$$\therefore x_{d(B)} = x_{d(A)} + \Delta t\left(\dot{x}_{d(A)} + \frac{\Delta t}{m_d}\left(k_w(x_{p(A)} - x_{d(A)}) - k_d x_{d(A)} - d_d\dot{x}_{d(A)}\right)\right)$$

Finally, by obtaining the displacement of drum brake spring x_d, the total braking force for the mechanical brake equation is;

$$F_{mechanical} = k_d x_{d(P)} - d_d\dot{x}_{d(P)} \tag{4}$$

Figure 6 shows the simulation model of the whole hydraulic-mechanical hybrid brake system. The master cylinder was modeled by a constant pressure

1.8 *MPa*. The power cylinder, front and rear drum brakes were modeled by spring-mass-damper models. The spring coefficient used was $k = 6.36 \times 10^7 N/m$ and the viscous damping coefficient was $d = 9.81 \times 10^2 Ns/m$. The wire connecting the link and rear drum brake was modeled also as a spring with coefficient of $k = 2.82 \times 10^8 N/m$.

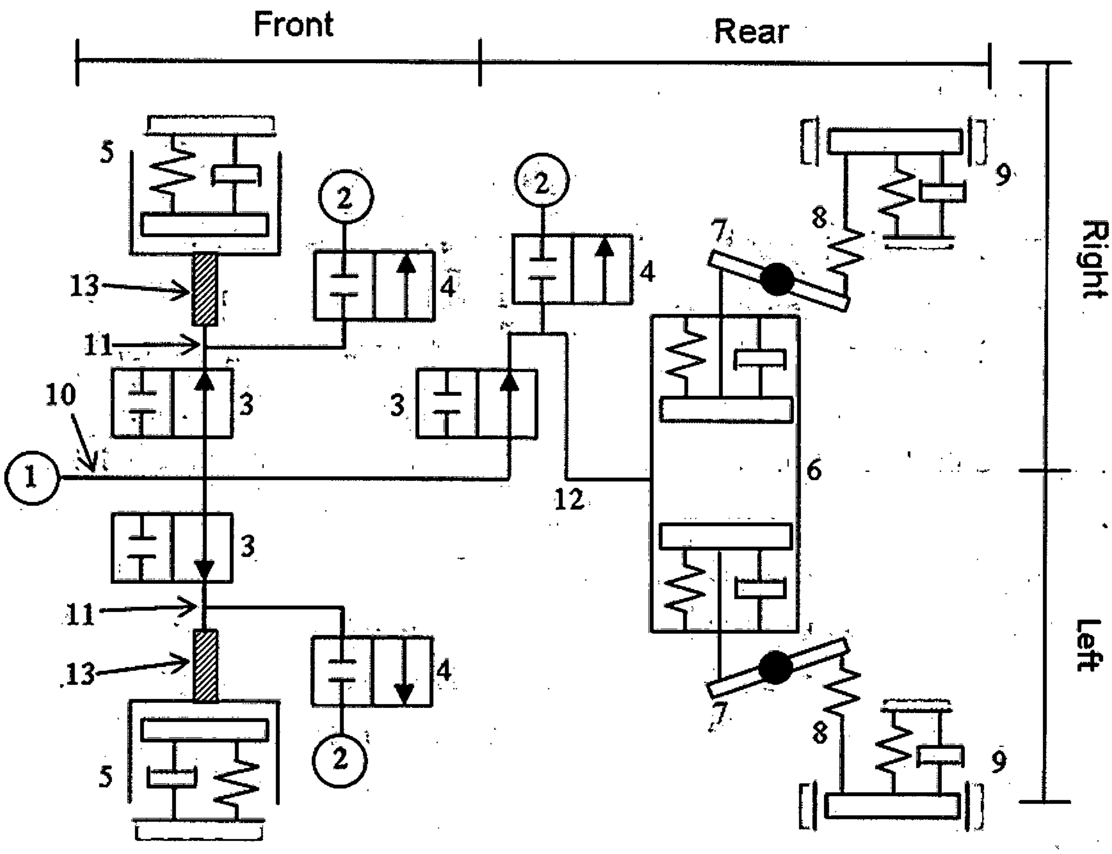

1:Master Cylinder 2:Low Pressure Source 3:In Valve 4:Out Valve 5:Front Drum Brake 6:Power Cylinder 7:Link 8:Wire 9:Rear Drum Brake 10:Master Cylinder Line 11:Front Hydraulic Line 12:Rear

Figure 6: Simulation Model

Regenerative Brake System

Regenerative braking is always related to vehicle that applies electric motor. Nearly all electric motors are based on magnetism. When an electric is directed to the stator and rotor, different magnetic poles are formed between them and give rise to a force which produces torque (kinetic energy). In reverse process or braking, the rotor is force to turn in opposite direction by the wheel's momentum that leads the motor to become an electric generator converting kinetic energy into output of electric energy. The electrical load produce make the braking effect on the vehicle.

From the mechanism of electric motor, it clearly understood that regenerative brake force is proportional to the rotational speed of the rotor; which in this case is the motor shaft. When the vehicle is in braking mode, the motor shaft turns the rotor in opposite direction causing electrical load. As the vehicle gradually to stop the rotational speed of the wheel decreases and so thus the electrical current produce. The declination of braking effect shows that the regenerative brake force diminished. In this research, the rear wheels are consisting of in-wheel motor and mechanical brake system. Figure 7 shows the ideal braking force and actual braking force to easily simulate the total force for rear brake system. Equation 5 is used to calculate the total amount of force on the rear tire.

$$F_{rear} = (\mathrm{C} \times \omega) + F_{mechanical} \qquad (5)$$

Where, F_{actual}: actual rear tire brake force, C: regenerative brake coefficient, ω: rotational speed of tire, and $F_{mechanical}$: mechanical brake force

Due to the rigidity of the mechanical brake system, a time delay during ABS operational occurs. Thus, to compensate the lost friction force, regenerative brake control timing is proposed. During ABS operational, if the slip ratio ρ surpass 0.3, then the regenerative brake is turn off and the current produced is transferred to charge the battery. However, if the slip ratio becomes lower than

0.2, regenerative brake is turned back on to regain the ideal brake force intended. The coefficient value of regenerative brake is 25 [Ns].

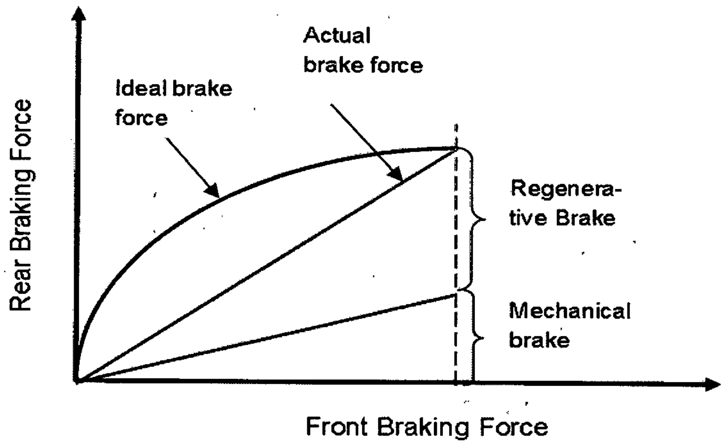

Figure 7: Ideal Braking Force Distribution

SIMULATION CONDITION

Vehicle Dynamic

In order to determine the velocity of front and side of the vehicle, basic dynamic motion equation is used. While for the cornering motion we used the basic equation of yaw rotation. Initial steer angle was set to 20^0 counter clock wise.

Figure 8 shows the modification of force vector for the construction of basic motion equation. Below are the equations of motion for longitude and traverse direction of the vehicle used in the simulation [(10)].

$$m\left(\frac{du}{dt} - v\Upsilon\right) = \left(-X_{fr} - X_{fl}\right)\cos\theta + \left(-Y_{fr} - Y_{fl}\right)\sin\theta - X_{rr} - X_{rl} \qquad (6)$$

$$m\left(\frac{dv}{dt} + u\Upsilon\right) = \left(Y_{fr} + Y_{fl}\right)\cos\theta + \left(-X_{fr} - X_{fl}\right)\sin\theta + Y_{rr} + Y_{rl} \qquad (7)$$

Where u, v donate the velocity of longitude, traverse axis, Υ is the vehicle yaw rotational speed, X_{fr}, X_{fl}, X_{rr}, X_{rl} are the friction force while Y_{fr}, Y_{fl}, Y_{rr}, Y_{rl} are the lateral force for each front and rear tire. Due to the fact that during cornering the front tires are tilted to an angle θ [deg], the friction force and lateral force have to be disintegrated into longitude and traverse direction of the vehicle. Below is the equation of yaw rotation:

$$\begin{aligned} I\frac{d\omega}{dt} &= l_f\left(Y_{fr}\cos\theta + Y_{fl}\cos\theta - X_{fr}\sin\theta - X_{fl}\sin\theta\right) - l_r(Y_{rr} + Y_{rl}) \\ &\quad + \frac{d_f}{2}\left(-X_{fr}\cos\theta + X_{fl}\cos\theta - Y_{fr}\sin\theta + Y_{fl}\sin\theta\right) \\ &\quad + \frac{d_r}{2}(-X_{rr} + X_{rl}) \qquad (8) \end{aligned}$$

Generally when a vehicle is moving in a straight direction, the heading direction of the wheel corresponds with the driving direction. Simply put that the wheel moving direction is linear to the wheel rotational plane. However, when the vehicle is steering and produce lateral as well as yaw motion, a displacement will occur. The out of alignment between the wheel moving direction and the rotational plane produce an angle which is define as side slip angle.

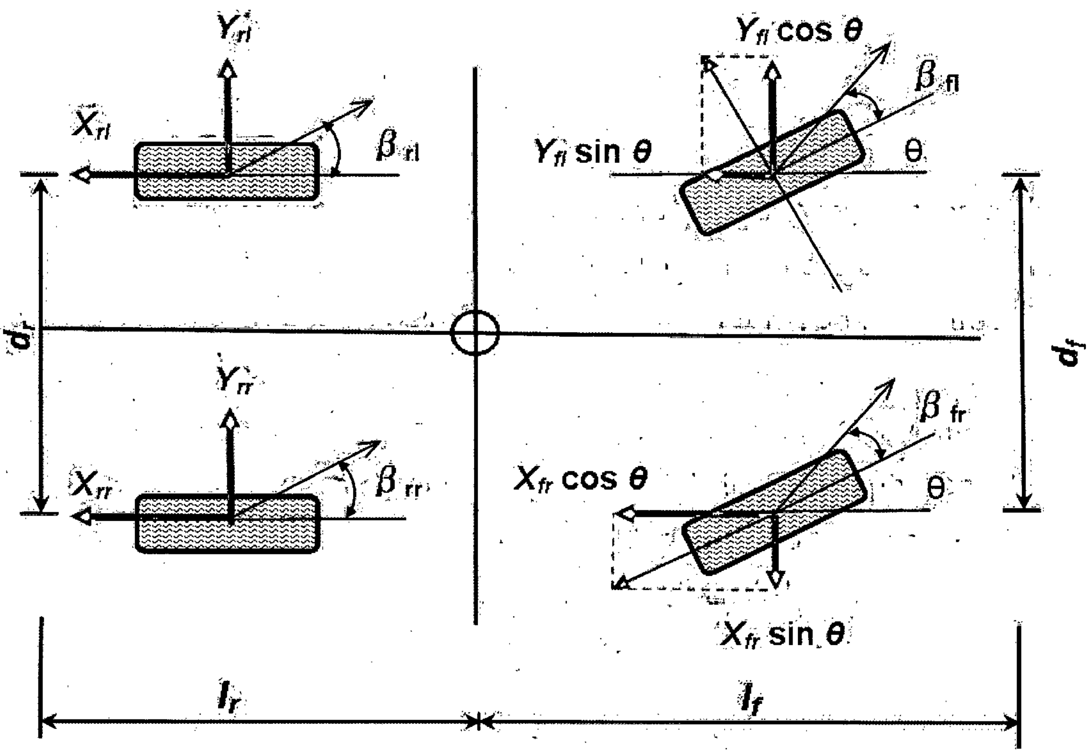

Figure 8: Modification of Force Vector

In figure 8, $\beta_{fr}, \beta_{fl}, \beta_{rr}, \beta_{rl}$ is the tire side slip angle. Consequently, each tire will have the velocity component of the center of gravity, and the velocity component due to rotation around the center of gravity. The heading of the front wheels has an angular displacement of θ degree, which is the actual steer angle of the driver, with respect to the longitude direction. The heading direction of the rear wheels are the same as the vehicle longitude direction. Therefore, the side slip angle for each tire can be written as below.

$$\beta_{fl} \approx \frac{V\beta + l_f r}{V - \frac{d_f r}{2}} - \delta$$

$$\beta_{fr} \approx \frac{V\beta + l_f r}{V + \frac{d_f r}{2}} - \delta$$

$$\beta_{rl} \approx \frac{V\beta - l_r r}{V - \frac{d_r r}{2}}$$

$$\beta_{rl} \approx \frac{V\beta - l_r r}{V + \frac{d_r r}{2}} \tag{9}$$

The lateral force and the friction force between interacting surface of tire and road surface equations are correlate with slip ratio, tire side slip angle and weight distribution is shown below. The model of deformation of tire tread rubber was also used to calculate these equations. In cases of braking situation we use Eq. (10a) while in driving situation Eq. (10b) is used. Moreover during braking, due to inertia at the center gravity point, a weight distribution at the longitude and to the side of the vehicle is put into consideration. So the tire weight W_z is already represented as weight distribution of each tire [11].

$$\xi_p = 1 - \frac{K_s \lambda}{3\mu W_z (1 - \rho)}$$

$$\lambda = \sqrt{\rho^2 + \left(\frac{K_\beta}{K_s}\right)^2 \tan^2 \beta_T}$$

$$K_s = \frac{b {l_T}^2}{2} K_x \quad , \quad K_\beta = \frac{b {l_T}^2}{2} K_y$$

$$Y \begin{cases} = -\dfrac{K_\beta \tan \beta_T}{1 - \rho} {\xi_p}^2 - 6\mu W_z \dfrac{K_\beta \tan \beta_T}{K_s \lambda} \left(\dfrac{1}{6} - \dfrac{1}{2} {\xi_p}^2 + \dfrac{1}{3} {\xi_p}^3\right) & (\xi_p > 0) \\ = -\mu W_z \dfrac{K_\beta \tan \beta_T}{K_s \lambda} & (\xi_p < 0) \end{cases}$$

$$X\begin{cases} = -\dfrac{K_s\rho}{1-\rho}{\xi_p}^2 - 6\mu W_z\dfrac{\rho}{\lambda}\left(\dfrac{1}{6}-\dfrac{1}{2}{\xi_p}^2+\dfrac{1}{3}{\xi_p}^3\right) & (\xi_p > 0) \\ = -\mu W_z\dfrac{\rho}{\lambda} & (\xi_p < 0) \end{cases}$$

(10a)

$$\xi_p = 1 - \frac{K_s\lambda}{3\mu W_z}$$

$$\lambda = \sqrt{\rho^2 + \left(\frac{K_\beta}{K_s}\right)^2 (1+\rho)^2 \tan^2\beta_T}$$

$$Y\begin{cases} = -K_\beta \tan\beta_T(1+\rho)\,{\xi_p}^2 - 6\mu W_z\dfrac{K_\beta \tan\beta_T\,(1+\rho)}{K_s\lambda}\left(\dfrac{1}{6}-\dfrac{1}{2}{\xi_p}^2+\dfrac{1}{3}{\xi_p}^3\right) & (\xi_p > 0) \\ = -\mu W_z\,\dfrac{K_\beta \tan\beta_T(1+\rho)}{K_s\lambda} & (\xi_p < 0) \end{cases}$$

$$X\begin{cases} = -K_s\rho{\xi_p}^2 - 6\mu W_z\dfrac{\rho}{\lambda}\left(\dfrac{1}{6}-\dfrac{1}{2}{\xi_p}^2+\dfrac{1}{3}{\xi_p}^3\right) & (\xi_p > 0) \\ = -\mu W_z\dfrac{\rho}{\lambda} & (\xi_p < 0) \end{cases}$$

(10b)

Where, *b*, *l:* width and length of interacted tire surface, K_x, K_y: stiffness of vertical and horizontal axis of tire. In this research, *b*=10 *cm*, *l*=15 *cm*, $K_x = 3.33 \times 10^7 N/m^3$,$K_y = 3.33 \times 10^7 N/m^3$ was set as constant.

Load Transfer Effect

As describe before, the tire friction force and the tire literal force changes with weight distribution of the tire. When there is a load transfer from rear tire to the front tire during braking, the sum of friction force for the front tire is much higher than the rear tire. This effect also implies during cornering where when there is a load transfer between the left and the right wheels, the sum of their lateral force will be lower than when load transfer is not considered.

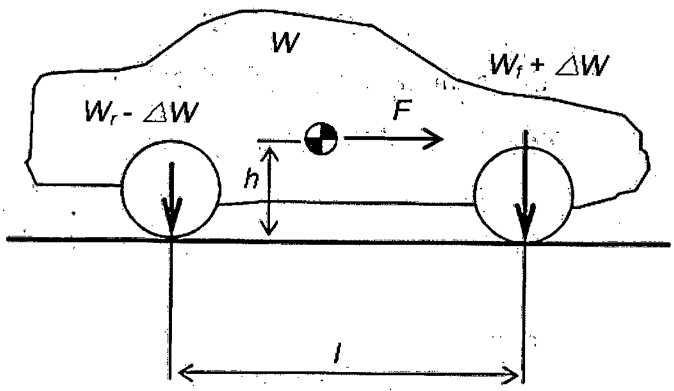

Figure 9: load transfer for braking

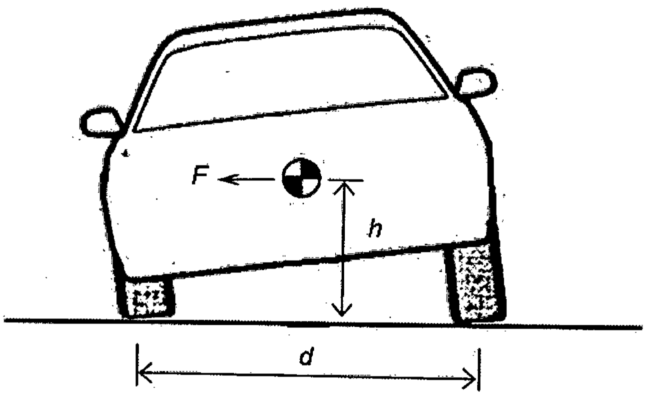

Figure 10: load transfer for cornering

Figure 9 is used to explain the load transfer for braking of a vehicle. There is an inertial force F acting to the front of the vehicle from the center gravity during braking. At that moment, consider that the moment around the rear wheel is balance by the moment due to the load transfer acting on the front wheel, and balance that moment to the moment of inertia force acting on the center of gravity, so the load transfer for braking is equal to;

$$l \times \Delta W = h \times F$$

$$l\Delta W = h \times \frac{W}{g} a$$

$$\therefore \Delta W_{braking} = \mathrm{W} \cdot \frac{a_X}{g} \cdot \frac{h}{l}$$

The same principle is used to calculate the load transfer cause by cornering. From figure 10, the inertia force is substitute with the centripetal force acting from the center gravity of the vehicle during cornering.

$$\therefore \Delta W_{cornering} = \mathrm{W} \cdot \frac{a_Y}{g} \cdot \frac{h}{d}$$

In the simulation, if considering that the vehicle is in the condition of braking and turning to the left, the most weight will concentrate on the front right wheel and the least weight will be at the rear left wheel. As a conclusion of the load transfer, the weight distribution of the vehicle during cornering and braking are shown below.

$$\begin{aligned} W_{fr} &= W_{fr} + \Delta W_{braking} + \Delta W_{cornering} \\ W_{fl} &= W_{fl} + \Delta W_{braking} - \Delta W_{cornering} \\ W_{rr} &= W_{rr} - \Delta W_{braking} + \Delta W_{cornering} \\ W_{rl} &= W_{rl} - \Delta W_{braking} - \Delta W_{cornering} \end{aligned} \tag{11}$$

VEHICLES TIRE STIFFNESS

Tires are one of the most important part of a vehicle as it is the only contact surface of the vehicle with the road. Type of tires can affect the maneuverability and performance of driving. In the calculation condition of the simulation, the stiffness of the tire's tread rubber plays a great deal on the outcome of the result. Thus, a simple experiment was done to determine the approximation value of the stiffness of the tire for the small in-wheel electric vehicle.

According to Equation (10a), (10b), the stiffness of the tire affects the friction force between the tire and the road surface. K_x, K_y represent the vertical and lateral stiffness of the tread rubber in unit width and length. In early hypothesis, in case of braking if the stiffness of the tire is higher, the friction force produced will relatively be higher and resulting in a shorter stopping time. On the other hand, if the stiffness of the tire is low, the friction force will be relatively small and a longer stopping time is expected. Due to inadequate equipment, an approximation of the stiffness value was performed by comparing the stopping time result by experiment and simulation.

Experimental methods for the K_x vertical stiffness:
A small in-wheel electric vehicle was driven in a straight line on dry asphalt until the velocity reaches a constant speed. A lever, which was installed earlier at the brake pedal to avoid human error, was pulled for braking. The velocity of the vehicle, rotational speed and braking pressure was recorded by speed sensors. The regenerative brake was off by letting the motor shift switch in 'neutral' mode (figure 11) to prevent additional variables. Similar condition (velocity, brake pressure, steer angle) is done by simulation and the stopping time result is then compared to the experimental result to obtain the approximate vertical stiffness of the tire.

Experimental methods for the K_y lateral stiffness:
A small in-wheel electric vehicle was driven in a constant steer angle until the velocity reaches a constant speed. The brake lever was pulled during braking. The velocity of the vehicle, rotational speed and braking pressure was recorded by speed sensors. The regenerative brake was off. Again, similar condition